# Forest Reflectance and Transmittance

# FRT User Guide

*Version 04.2013*

A. Kuusk and T. Nilson

Tartu Observatory

2013

# Contents

# Abstract

A directional multispectral forest reflectance model has been developed in the group of vegetation remote sensing at Tartu Observatory, Estonia. The early version of the forest reflectance model by Nilson (1991) has been extensively modified. The modified leaf optics models PROSPECT by Jacquemoud et al. (1996) and LIBERTY by Dawson et al. (1998), atmosphere radiative transfer model 6S by Vermote et al. (1994, 1997), and homogeneous two-layer canopy reflectance model ACRM by Kuusk (2001) have been incorporated into the model. The new model works in the spectral region 400-2400 nm with the same set of input parameters, the spectral resolution is 1 nm. Any Sun and view directions are allowed. The following manual presents the Fortran-77 code of the model.

# 1 Introduction

The transfer of solar radiation within forest stands is a rather complex process. We need models to understand how the reflected signal is formed and which are its most important driving factors. In addition, to create a satellite or aerial imagery-based forest management system, forest reflectance models capable of acting as an interface between the images and forestry databases are required. These models should be able to make maximum use of the forestry data contained in the database and allow to simulate the optical images, e.g. in terms of standwise ground-level reflectance factors. Originally, the forest reflectance model described in Nilson and Peterson (1991) has been derived just from these starting points. The previous version of the model needed several improvements. First of all, to make use of multiangular remote sensing data, the model should be modified into a multiangular version. Second, a multispectral version of the model is required to study the relations between leaf biochemical and high spectral resolution reflectance data. Several improvements were also needed to create a more user-friendly version of the model and to introduce some changes in the calculation algorithm. For these purposes, a considerable modification of the original model was undertaken.

# 2 General layout of the model

The forest reflectance model may be classified as a hybrid-type model, including the properties both geometrical and radiative transfer equation-based models. Tree crown envelopes are modeled as ellipsoids of rotation or cones in the upper and cylinders in the lower part (Fig. 1). Leaves and branches are uniformly distributed in the crown and spherically oriented.

Several tree classes of different size and/or species are possible (Fig. 1). Within each class, trees are considered identical.

A homogeneous layer of vegetation is present on the ground surface.

The radiances of the forested scene components – tree leaves/needles, branches and stems, ground vegetation, and soil – are estimated with the help of geometrical and radiative transfer concepts. Special attention is paid to the adequate modeling of single scattering reflectance components, whereas reflectance caused by multiple scattering of radiation in the canopy is more roughly modeled.

The directional spectral reflectance of a forest stand in the given direction $r_2$ is calculated as a sum of the single scattering reflectance $\rho_I(r_1, r_2)$ and diffuse reflectance $\rho_D(r_2)$,

$$\rho(r_1, r_2) = \frac{I_\lambda}{Q_\lambda}\rho_I(r_1, r_2) + \rho_D(r_1, r_2)\,, \tag{1}$$

where $I_\lambda = I_\lambda(\theta_1)\,cos(\theta_1)$ is direct down-welling flux, and $Q_\lambda = I_\lambda + D_\lambda$ is the total down-welling flux, $D_\lambda$ is diffuse downwelling flux, $r_1$ and $r_2$ are unit vectors in the Sun and view direction, respectively, $\theta_1$ is the Sun zenith angle.

The single scattering reflectance factor $\rho_I(r_1, r_2)$ accounts for the single scattering from tree layer foliage and stems $\rho^1_{CR}(r_1, r_2)$, and single scattering from ground vegetation $\rho^1_{GR}(r_1, r_2)$,

$$\rho_I(r_1, r_2) = \rho^1_{CR}(r_1, r_2) + \rho^1_{GR}(r_1, r_2). \tag{2}$$

Diffuse reflectance $\rho_D(r_1, r_2)$ accounts both for the multiple scattering of radiation and for the diffuse radiance of scattered/reflected sky radiation $D_\lambda$.

The model works in the optical domain of radiation, 400-2400 nm, spectral resolution is 1 nm.

# 3 Model components

## 3.1 Single scattering on tree crowns

The first-order reflectance component $\rho^1_{CR}(r_1, r_2)$ is calculated separately for all tree classes,

$$\begin{aligned}
\rho^1_{CR}(r_1, r_2) &= \sum_{j=1}^{m} \rho^1_{CRj}, \\
\rho^1_{CRj} &= \lambda_j \iiint\limits_{V_j} u_j\, \Gamma_j(r_1, r_2)\, p_{00j}(x, y, z; r_1, r_2)\, dxdydz / \cos\theta_1
\end{aligned} \tag{3}$$

Here $\lambda_j$ is the number of trees of the $j$ th class per unit ground area, $u_j = u_j(x, y, z)$ is the foliage area volume density within a tree crown, $\Gamma_j(r_1, r_2)$ is the scattering (area) phase function

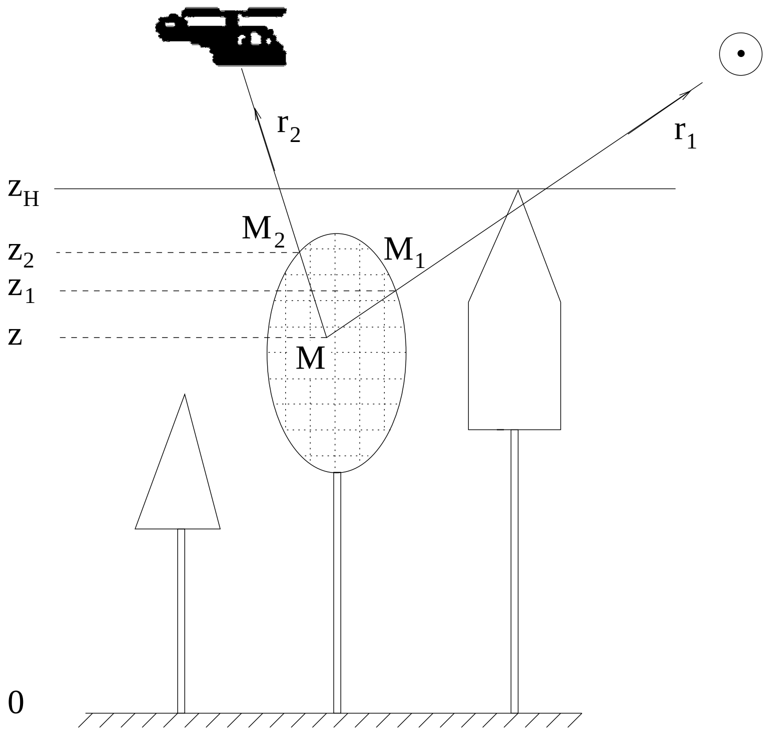


Figure 1: Deriving the first-order scattering component.

of the canopy medium, $p_{00j}()$ is the bidirectional gap probability of two simultaneous free lines-of-sight in directions $r_1$ and $r_2$ from the point $M = (x, y, z)$ within a crown of the $j$ th tree class (Fig. 1), $V_j$ is the spatial region corresponding to the crown envelope. Integral (3) is calculated numerically.

The scattering phase function $\Gamma_j(r_1, r_2)$ in formula (3) is the sum of diffuse $\Gamma_{j,D}(r_1, r_2)$ and specular $\Gamma_{j,sp}(r_1, r_2)$ scattering,

$$\Gamma_j(r_1, r_2) = \Gamma_{j,D}(r_1, r_2) + \Gamma_{j,sp}(r_1, r_2). \tag{4}$$

Leaves of broadleaf species are supposed to be bi-Lambertian, foliage element reflection $\rho_{Lj}$ and transmission $\tau_{Lj}$ coefficients are calculated with PROSPECT submodel (Jacquemoud and Baret, 1990). Leaf refractive index $n_{Lj}$ is a given tabulated function of wavelength. Foliage orientation is described by the two-parameter elliptical leaf angle distribution (LAD) (Kuusk, 1995a),

$$g_L(\theta_L) = B_g/\sqrt{1 - \epsilon^2 \cos^2(\theta_L - \theta_m)}, \tag{5}$$

where $\theta_L$ is leaf inclination, $\theta_m$ is the modal leaf inclination, and $\epsilon$ is the eccentricity of the LAD which determines the shape of the LAD, $B_g$ is a normalizing factor. As the sensitivity range on the LAD eccentricity is very close to the limit value $\epsilon = 1$, the parameter $e_L = -\log(1-\epsilon)$ is used as the input parameter of FRT.

On these assumptions, the scattering phase function $\Gamma_{j,D}(r_1, r_2)$ in Eq. (4) may be calculated by analytical formulas in case of a few exceptional LAD (spherical, horizontal, vertical LAD, or fixed leaf angle) (Nilson, 1991), or by approximation formulae in case of elliptical LAD (Kuusk, 1995a).

For conifer species the asymmetric Henyey-Greenstein phase function is used (Lenoble, 1977),

$$\Gamma_{HG}(\gamma) = \frac{1-g^2}{\sqrt{(1+g^2-2\,g\,\cos(\gamma))^3}}, \tag{6}$$

where $g$ is the asymmetry parameter, $-1 \leq g \leq 1, \gamma$ is the angle between sun and view directions.

Optical parameters are averaged over all foliage elements (leaves, branches) according to their share in the total foliage area.

The bidirectional gap probability $p_{00j}$ is defined as a product of two independent probabilities

$$p_{00j} = p_1\, p_2 \tag{7}$$

$p_1$ being the within-crown level bidirectional gap probability and $p_2$ that of the between-crown level. In calculations of the bidirectional gap probability $p_1$, results from (Kuusk, 1991) for the crown of a single tree are applied. The mutual shading of needles in shoots and the characteristic linear dimension of foliage elements $l_{sh}$ are accounted for.

The between-crown gap probability, $p_2$, in Eq. (7) stands for the parts of the lines-of-sight that lie outside the crown of interest, i.e. from the point $M_1(x_1, y_1, z_1)$ until the upper boundary of the forest canopy in the solar direction and from $M_2(x_2, y_2, z_2)$ in the view direction (Fig. 1). Based on (Nilson, 1977) it is calculated as follows:

$$p_2 = a_s(z_1, \theta_1)\, a_s(z_2, \theta_2)\, C_{HS2}(z_1, z_2, l_{12}, r_1, r_2)\,, \tag{8}$$

where $a_s(z, \theta)$ is the average proportion of gaps in the forest canopy at the height $z$ in the direction $\theta$, and $C_{HS2}$ is the hot-spot correction factor for between-crown shading,

$$C_{HS2}(z_1, z_2, l_{12}, r_1, r_2) = \exp\left[\sum_j \lambda_j c_j S_{cj}(z_1, z_2, l_{12}, r_1, r_2)\, p_{0j}\right]\,, \tag{9}$$

$S_{cj}(z_1, z_2, l_{12}, r_1, r_2)$ is the area of the common part of the $j$ th class crown envelope projections in solar and view directions, corresponding to the heights $z_1$ and $z_2$ and the horizontal distance

$l_{12}$; $p_{0j}$ is the joint probability of gap occurrence within a single $j$ th class tree crown when viewed simultaneously from a point at the height $z_1$ in the solar direction $r_1$ and from another point at the height $z_2$ in the view direction $r_2$, horizontal distance of the points being $l_{12}$. The parameter $c_j$ is introduced to account for the deviations in the tree distribution pattern from the Poisson distribution, see Eq. (17).

The gap probability $a_s(z, \theta)$ is calculated on the assumption of the binomial distribution of trees (Nilson, 1977),

$$a_s(z, \theta_r) = \exp\left\{ -\sum_j \lambda_j [b_{1j}(z, \theta_r) S_{crown,j}(z, \theta_r) + S_{trunk,j}(z, \theta_r)] \right\} , \tag{10}$$

where $b_{1j}(z, \theta_r) = \ln[1-(1-a_{1j}(z, \theta_r))(1-c_j)]/(1-c_j)$, $S_{crown,j}(z, \theta_r)$ is the area of crown envelope projection for class $j$ at the level $z$, and $S_{trunk,j}(z, \theta_r)$ is the area of trunk projection for class $j$ at the level $z$, $a_{1,j}(z, \theta_r)$ is the gap probability in crowns of the tree class $j$ in the direction $\theta_r$ at the level $z$, $\theta_r$ is the polar angle of the view vector $r_i, i = 1, 2$. The area of trunk projection $S_{trunk,j}(z, \theta_r)$ is calculated using trunk tapering curves by Ozolins (1988). The function $a_{1j}(z, \theta_r)$ is shown in Eq. (11),

$$a_{1j}(z, \theta_r) = exp(-u_j\, G(\theta_r) \frac{V_j(z)}{S_{crown,j}(z, \theta_r) \cos(\theta_r)}) , \tag{11}$$

$V_j(z)$ is the volume of the tree crown above the level $z$ in the tree class $j$, $G(\theta_r)$ is the Ross-Nilson geometry function. In case of spherical LAD $G(\theta_r) = 1/2$, for other LAD-s the approximation by Kuusk (1995a) are used. As the crown envelopes are supposed to be surfaces of revolution, the between-crown gap probability $a_s(z, \theta_r)$ does not depend on the azimuth. Grouping and/or regularity of the stand is described by a grouping parameter $c_j$ in every tree class, $c_j < 1$, $c_j = 1$, and $c_j > 1$ correspond to a regular, random, and clumped pattern of trees in class $j$, respectively. As the stem coverage (basal area) is very small, unlike the crowns, the stem displacement pattern is supposed to be random.

In Eq. (10), the expression $\lambda_j[S_{crown,j}(z, \theta_r) + S_{trunk,j}(z, \theta_r)]$ stands for the mean coverage of ground by the shadows cast by crown envelopes and trunks from tree class $j$, if the direction of sunrays coincide with the view direction $\theta_r$. It is the effective coverage that should appear in the exponent of Eq. (10). The mean coverage should be diminished, because the tree crowns are supposed to be semi-transparent, and modified to account for the tree distribution pattern effect. The two effects of single-crown transparency and of the tree distribution pattern on the between-crown canopy gap fraction are introduced by the parameter $b_{1j}(z, \theta_r)$. Note that $b_{1j}(z, \theta_r) = 1 - a_{1,j}(z, \theta_r)$, if $c_j = 1$.

The overlapping of crown projections in Sun and view directions $S_{cj}()$, which is needed for the calculation of between-crown level bidirectional gap probabilities, is calculated so that the

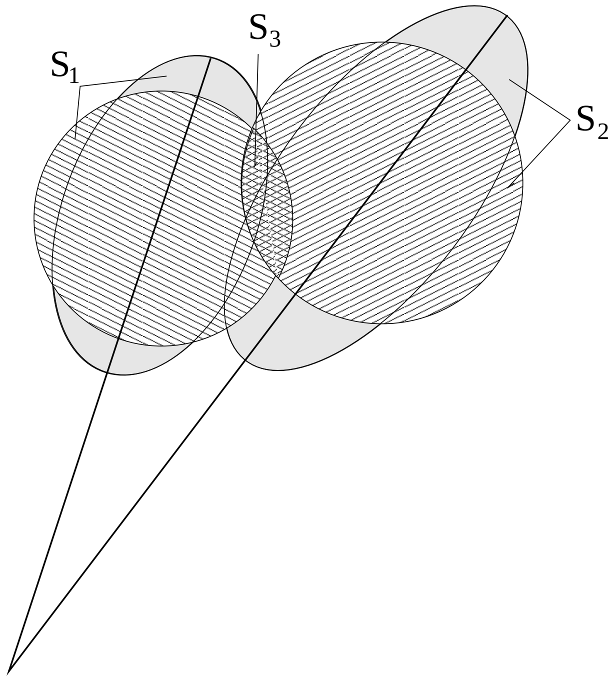


Figure 2: Calculation of the overlapping of crown projections.

crown projections $S_1$ and $S_2$ in Sun and view directions, respectively, are substituted with circles of the same area. Centers of the circles are halfway between the projections of the base and the top of a crown, see Fig. 2. The estimated overlapping area $S_3$ in Fig. 2 may be biased to some extent. Depending on the Sun and view angles, the relative azimuth between Sun and view directions, and the tree height and the crown size, both over- and underestimation of the overlapping area $S_3$ are possible.

## 3.2 Single scattering on ground vegetation

The two-layer homogeneous canopy reflectance model ACRM by Kuusk (2001) is applied for the calculation of the bidirectional reflectance of ground vegetation. Input parameters of the ACRM are the leaf area index (LAI), leaf size, two leaf angle distribution parameters, the set of biophysical parameters (PRSOPECT or LIBERTY parameters) for two layers of ground vegetation, and weights of Price's functions for the calculation of the soil reflectance spectrum. The probability of seeing sunlit ground vegetation is calculated as the $p_2$ in Eq. (8) for the ground surface, $z_1 = z_2 = l_{12} = 0$.

### 3.3 Diffuse fluxes

Diffuse fluxes of multiple scattering and of diffuse sky radiation are considered in four flux approximation like in the SAIL model (Verhoef, 1984) and in the ACRM model (Kuusk, 2001). Four differential equations define four fluxes: vertical fluxes up $E_+$ and down $E_-$, a direct solar flux $E_s$, and a flux associated with the radiance in the direction of observation $E_o$,

$$\begin{aligned} dE_+/dz &= -au_L E_+ + \sigma u_L E_- + s' u_L E_s \\ dE_-/dz &= -\sigma u_L E_+ + au_L E_- - su_L E_s \\ dE_s/dz &= ku_L E_s \\ dE_o/dz &= vu_L E_- + uu_L E_+ - Ku_L E_o \end{aligned} \tag{12}$$

The SAIL coefficients $a$, $\sigma$, $s'$, $s$, $k$, $v$, $u$, and $K$ are expressed using the G-function and leaf reflection and transmission coefficients $\rho_L$ and $\tau_L$. Equations (12) can be solved analytically, the general solutions for $E_+$, $E_-$ and $E_s$ are given, e.g. in (Bunnik, 1978).

The diffuse component of reflectance $\rho_d$ is a sum of two components, related to tree layer and to ground vegetation, $\rho_d^{\rm trees}$ and $\rho_d^{\rm gr}$, respectively,

$$\rho_d = \rho_d^{\rm trees} + \rho_d^{\rm gr}, \tag{13}$$

where

$$\begin{aligned} \rho_d^{\rm trees} &= {\rm SQ}\, r_{so} + (1 - {\rm SQ})\, r_{do} + \\ &+ [{\rm SQ}\,(p_1\, r_{sd}^{\rm gr} + t_{sd}\, r_{dd}^{\rm gr}) + (1 - {\rm SQ})\, t_{dd}\, r_{dd}^{\rm gr}]\, t_{do} \,/\, (1 - r_{dd}\, r_{dd}^{\rm gr}) \end{aligned} \tag{14}$$

and

$$\rho_d^{\rm gr} = [{\rm SQ}(p_1\, r_{sd}^{\rm gr}\, r_{dd} + t_{sd}) + (1 - {\rm SQ})\, t_{dd}] r_{ds}^{\rm gr}\, p_2 \,/\, (1 - r_{dd}\, r_{dd}^{\rm gr}). \tag{15}$$

Here SQ $= I_\lambda/Q_\lambda$, $p_i = p(r_i)$ is the gap probability in direction $r_i$, $r_{sd}^{\rm gr}$, $r_{ds}^{\rm gr}$ and $r_{dd}^{\rm gr}$ are the directional-hemispherical, hemispherical-directional, and hemispherical-hemispherical reflectance of ground vegetation, respectively. The ground vegetation reflectances $r_{sd}^{\rm gr}$, $r_{ds}^{\rm gr}$, and $r_{dd}^{\rm gr}$ are calculated by integrating the ACRM model over hemisphere by view, incident, and both directions, respectively.

The scattering operators of the tree layer $r_{so}, r_{do}, t_{do}, t_{sd},$ and $t_{dd}$ are defined in Table 1 where $D_\lambda = Q_\lambda - I_\lambda$.

When calculating diffuse fluxes, the plant material is supposed to be distributed homogeneously in the horizontal, no layers, no trees, no branches, no shoots, and driving parameters are determined as averages approximating the behavior of the canopy in bulk. The effective foliage area

Table 1: Scattering operators of the tree layer

| Definition | Boundary conditions | | | |
|---|---|---|---|---|
| $r_{dd} = E_+(0)/E_-(0)$ | $E_s(0) = 0,$ | $E_+(-1) = 0,$ | $E_-(0) = D_\lambda$ | |
| $t_{dd} = E_-(-1)/E_-(0)$ | $E_s(0) = 0,$ | $E_+(-1) = 0,$ | $E_-(0) = D_\lambda$ | |
| $r_{sd} = E_+(0)/E_s(0)$ | $E_s(0) = I_\lambda,$ | $E_+(-1) = 0,$ | $E_-(0) = 0$ | |
| $t_{sd} = E_-(-1)/E_s(0)$ | $E_s(0) = I_\lambda,$ | $E_+(-1) = 0,$ | $E_-(0) = 0$ | |
| $r_{do} = E_o(0)/E_-(0)$ | $E_s(0) = 0,$ | $E_+(-1) = 0,$ | $E_-(0) = D_\lambda$ | |
| $t_{do} = E_o^-(-1)/E_-(0)$ | $E_s(0) = 0,$ | $E_+(-1) = 0,$ | $E_-(0) = D_\lambda,$ | $E_o^-(0) = 0$ |
| $r_{so} = E_o(0)/E_s(0)$ | $E_s(0) = I_\lambda,$ | $E_+(-1) = 0,$ | $E_-(0) = 0,$ | $E_o(-1) = 0$ |

index value $LAI_{eff}$ is used in the calculations of diffuse fluxes. $LAI_{eff}$ is calculated from the gap probability in a given direction, it depends on the G-function of foliage and on the tree distribution pattern (clumping/regularity). As the G-function is almost invariant relative to leaf orientation at zenith angle 40° (Ross and Nilson, 1968), the effective LAI is calculated from the gap fraction at $\theta_0 = 40°$,

$$LAI_{eff} = \frac{\sum_j (\kappa_{cl,j} LAI_j + BAI_j)}{\Omega_E}\,, \tag{16}$$

where

$$\begin{aligned} \Omega_E &= \frac{\sum_j (\kappa_{cl,j} LAI_j + BAI_j)}{\cos\theta_0 \sum_j \lambda_j S_{crown,j}(\theta_0) c_j(\theta_0)}\,, \\ c_j(\theta_0) &= \frac{\ln\left(1 - (1 - a_{1j}(\theta_0))\,(1 - GI_j)\right)}{1 - GI_j}\,. \end{aligned} \tag{17}$$

Here $\kappa_{clump,j}$ is the clumping coefficient of leaves/needles in a shoot of the tree class $j$, $BAI_j$ is the branch area index, $\theta_1$ is the Sun zenith angle, and $a_{1j}(\theta_1)$ is the gap probability in the Sun direction in crowns of the tree class $j$, $GI_j$ is the Fisher's grouping index - the relative variance of the number of trees in the area $S_{crown,j}(\theta)$. The effective value of the foliage area index $LAI_{eff}^{(mult)}$ is calculated from the assumption that the gap fraction in the direction of sunrays as calculated by means of Eq. (10), and the modified exponential formula, as proposed in Chen and Cihlar (1996), should be equal. Thus, $\Omega_E$ could be interpreted as the 'clumping index caused by structures larger than a shoot'.

### 3.4 Leaf optics

Leaf optics models PROSPECT (Jacquemoud and Baret, 1990) or LIBERTY (Dawson et al., 1998) can be used for the calculation of leaf reflectance and transmittance. Both these models are modified so that the number of leaf constituents and names of files of their extinction spectra are listed in the input file. Extinction spectra of the models PROSPECT2 (Jacquemoud et al., 1996), PROSPECT3 (Fourty and Baret, 1998), and LIBERTY (Dawson et al., 1998) are available. The structure parameter of a single leaf in the PROSPECT model $N$ is corrected to an effective value $N_{eff}$ in order to account for the clumping of leaves/needles into a shoot,

$$N_{eff} = N/\kappa_{cl} \,. \tag{18}$$

If compared with the PROSPECT model, the LIBERTY model has two additional parameters: average internal cell diameter and intercellular air space determinant (Dawson et al., 1998).

**In the forest model input, the biochemical parameters are expressed as a fraction of the dry matter of leaves/needles.** Using the described set of biophysical parameters, the whole spectrum of leaf reflectance and transmittance in the spectral range 400-2400 nm is calculated with the spectral resolution of 1 nm.

No good optical model for branch and trunk bark reflectance is available so far. Therefore, reflectance spectra of branch and trunk reflectance for every tree class are tabulated in separate input files.

### 3.5 Sky radiation

The wavelength-dependent relative share of direct and diffuse flux in incoming radiation is needed, Eq. (1). The atmospheric radiative transfer model 6S by Vermote et al. (1997) is involved for the calculation of incident radiation fluxes. Input parameters of the 6S model, which are needed for the calculation of down-welling fluxes, are the percentage of four main aerosol components (dust-like, oceanic, water-soluble, and soot), and horizontal visibility or aerosol optical thickness at 550 nm $\tau_{aer}^{550}$. The calculation of hemispherical-directional forest reflectance for sky radiation $\rho_D$ is simplified. Instead of double integration over the hemisphere for incident directions, integration is performed in the perpendicular plane ($\varphi = 90°$) only,

$$\rho_D(r_2) = \frac{\int_{2\pi} d(r_1)\rho_I(r_1, r_2)\mu_1 dr_1}{D_\lambda} \approx \frac{\int_0^{\pi/2} d(\theta_1, \varphi = \pi/2)\rho_I(\theta_1, \theta_2, \varphi = \pi/2)\mu_1 d\theta_1}{D_\lambda} , \tag{19}$$

where $d(r_1)$ is the sky radiance in the direction $r_1 = (\theta_1, \varphi_1)$, $\mu_1 = \cos\theta_1$, and $D_\lambda = \int_{2\pi} d(r_1)\mu_1 dr_1$ is the diffuse down-welling flux from the sky.

# 4 Transmittance of a forest canopy

The same algorithms can be used for the calculation of downward radiances and fluxes under a forest canopy. The relative downward radiance in direction $r_2$ Sun being in direction $r_1$ is presented as the sum of three components:

$$t(r_1, r_2) = t^1_{CR}(r_1, r_2) + t_{sky}(r_1, r_2) + t^M_{CR}(r_1, r_2)\,. \tag{20}$$

Here the downward radiance $t(r_1, r_2)$ is normalized as reflectance in Eqs (2, 1), $t^1_{CR}(r_1, r_2)$ is the radiance of single scattering from tree crowns, $t_{sky}(r_1, r_2)$ is the sky radiance, and $t^M_{CR}(r_1, r_2)$ is the radiance of multiple scattering on crowns. In the model the sky radiance $t_{sky}()$ depends only on the Sun zenith angle $\theta_1$.

Total transmittance of the tree layer $t_Q(r_1, r_2)$ is calculated as a ratio of the downward flux below the tree canopy to the incoming total flux $Q_\lambda$,

$$t_Q(r_1) = \frac{I}{Q_\lambda}\Big(t^I_{CR}(r_1) + a_s(0, \theta_1)\Big) + \frac{D_\lambda}{Q_\lambda}\int_{2\pi}\Big(a_s(0, r_2) + t^I_{CR}(r_2)\Big)\,\cos(\theta_2)\,dr_2\,, \tag{21}$$

and diffuse transmittance of the tree layer $t_D(r_1)$ is calculated as a ratio of the downward flux below the canopy (direct sunrays screened) to the incoming diffuse flux $D_\lambda$,

$$t_D(r_1) = \int_{2\pi}\Big(a_s(0, r_2)\cos(\theta_2) + t^I_{CR}(r_2)\Big)\,\cos(\theta_2)\,dr_2 + \frac{I_\lambda}{D_\lambda}t^I_{CR}(r_1)\,. \tag{22}$$

Here $t^I_{CR}(r)$ is the scattering operator $I_\lambda(r) \rightarrow$ (downward scattered flux) for tree crowns.

# 5 Inversion of the model

Inversion of the model can be performed similar to Goel and Strebel (1983) or Kuusk (1991): a merit function is built, which has its minimum value when the best fit of measured and calculated reflectance data is reached. This way the complicated task of the solution of an array of non-linear equations for the estimation of model parameters is reduced to a more simple problem of the search of an extremum of a multidimensional function. In the merit function constraints are used in order to avoid the non-physical values of input parameters, and uncertainties of reflectance data and an expert estimate of parameter values are accounted for,

$$F(X) = \sum_{j=1}^{m}\left(\frac{\rho^*_j - \rho_j}{\epsilon_j}\right)^2 + \sum_{i=1}^{n}\left[(x_i - x_{i,b})^4\,w_i^2 + \left(\frac{x_i - x_{e,i}}{dx_i}\right)^2\right]\,. \tag{23}$$

Here $X = (x_1, x_2, ..., x_n)$ is the vector of model input parameters, $m$ is the number of the measured reflectance values $\rho_j^*$, $\rho_j$ is the model reflectance value, $\epsilon_j$ is the error of the measured reflectance value $\rho_j^*$, $x_i$ is a model parameter and $x_{i,b}$ its value on the boundary of the given region; $w_i$ is a weight, $w_i = 0$ in the given region $x_i \in [x_{i,min}, x_{i,max}]$ and $w_i =$ const else, $x_{e,i}$ is the expert estimate of the parameter $x_i$, and $dx_i$ is a tolerance for the parameter $x_i$ which controls the sensitivity of the merit function on the expert estimate.

There is an option to use only absolute differences $(\rho_j^* - \rho_j)^2$ in the merit function.

In the inversion, the redundancy of data can be effectively used, i.e. the number of reflectance values inverted may be more than the number of model parameters subject to estimation. Anyway, as the number of model parameters is large, most of the model parameters should be fixed at 'best guess' values, and only a few parameters can be estimated simultaneously. Only the parameters of the first tree class can be estimated in the inversion.

# 6 Conclusion

The model can be used for the interpretation of multispectral and/or multiangular remote sensing data in the wide range of Sun and view angles in the whole optical domain 400-2400 nm. The proposed version of the model seems to be a good tool for different sensitivity analyses, e.g. an analysis of the dependence of BRDF, in particular near the hot spot, on the stand structural variables at different structural levels and on optical parameters of the canopy and understorey can be made.

The same computer code can be used both for direct and inversion modeling.

The model is coded in Fortran-77. The computational aspects of the model are detailed in the following appendices:

- General description of the computer code
- Example of inputs and outputs
- Complete description of the subroutines

## Acknowledgements

The first version of the model was coded by Mrs. Anne Jõeveer. The Fortran text of the PROSPECT model was provided by Dr. S. Jacquemoud, the C text of the LIBERTY model was provided by Dr. T. Dawson, and the source text of the 6S model by Dr. E. Vermote. Absorption spectra for the PROSPECT model were provided by Dr. F. Baret.

# References

Bunnik, N.J.J., 1978. *The Multispectral Reflectance of Shortwave Radiation by Agricultural Crops in Relation with their Morphological and Optical Properties*, Mededelingen Landbouwhogeschool, Wageningen, The Netherlands, 175 pp.

Chen, J.M. and Cihlar, J., 1996. Retrieving leaf area index of boreal conifer forests using Landsat TM images, *Remote Sens. Environ.*, 55(2):153-162.

Dawson, T.P., Curran, P.J., and Plummer, S.E., 1998. LIBERTY - modeling the effects of leaf biochemical concentration on reflectance spectra. *Remote Sens. Environ.* 65:50-60.

Fourty, T. and Baret, F., 1998. On spectral estimates of fresh leaf biochemistry. *Int. J. Remote Sens.* 19:1283-1297.

Goel, N.S. and Strebel, D.E., 1983. Inversion of vegetation canopy reflectance models for estimating agronomic variables. I. Problem definition and initial results using the Suits model. *Remote Sens. Environ.* 13:487-507.

Jacquemoud, S., and Baret, F., 1990. PROSPECT: A model of leaf optical properties spectra. *Remote Sens. Environ.* 34:75-91.

Jacquemoud, S, Ustin, S.L, Verdebout, J, Schmuck, G, Andreoli, G, and Hosgood, B., 1996. Estimating leaf biochemistry using the PROSPECT leaf optical properties model. *Remote Sens. Environ.* 56:194–202.

Kimes, D.S., Knyazikhin, Y., Privette, J.L., Abuelgasim, A.A., and Gao, F., 2000. Inversion methods for physically-based models. *Remote Sens. Reviews*, 18(2-4):381-439.

Kuusk, A., 1991. The hot spot effect in plant canopy reflectance. In: Myneni RB, Ross J, editors. *Photon-vegetation interactions. Applications in optical remote sensing and plant ecology.* Berlin: Springer, 139-159.

Kuusk, A., 1994. A multispectral canopy reflectance model. *Remote Sens. Environ.* 50:75-82.

Kuusk, A., 1995a. A fast, invertible canopy reflectance model, *Remote Sens. Environ.* 51(3): 342-350.

Kuusk, A., 2001. A two-layer canopy reflectance model, *J.Q.S.R.T.*, 71:1-9.

Kuusk, A., 1995b. A Markov chain model of canopy reflectance. *Agricult. Forest Meteorol.* 76:221-236.

Kuusk, A. and Nilson, T., 2000. A directional multispectral forest reflectance model. *Remote Sens. Environ.* 72(2):244-252.

Nilson T., 1977. A theory of radiation penetration into nonhomogeneous plant canopies. *The Penetration of Solar Radiation into Plant Canopies,* Acad. Sci. ESSR Report, Tartu, pp. 5-70. (Russian)

Nilson T., 1991a. Approximate analytical methods for calculating the reflection functions of leaf canopies in remote sensing applications. In: Myneni RB, Ross J, editors. *Photon-Vegetation Interactions. Applications in Optical Remote Sensing and Plant Ecology.* Berlin, Springer, 161-190.

Nilson T., and Peterson U., 1991b. A forest canopy reflectance model and a test case. *Remote Sens. Environ.* 37(2):131-142.

Ozolins, 1988: Standards for Forest Taxation in Latvia. Latvian Ministry of Forest Production and Management, Riga, 174 pp. (in Russian).

Press, W.H., Teukolsky, S.A., Vetterling, W.T., and Flannery, B.P., 1992. *Numerical Recipes in FORTRAN. The Art of Scientific Computing.* Cambridge University Press, Cambridge, 963 pp.

Ross, J., 1981. *The Radiation Regime and Architecture of Plant Stands.* Dr. W.Junk Publishers, The Hague, 391 pp.

Ross, J. and Nilson, T., 1968. The calculation of photosynthetically active radiation in plant communities. In: *Regime of the Solar Radiation in a Vegetation Canopy,* Inst. Phys. and Astronomy, Acd. Sci. Est. SSR, 5-54.

Verhoef, W., 1984. Light scattering by leaf layers with application to canopy reflectance modeling: the SAIL model. *Remote Sens. Environ.* 16:125-141.

Vermote, E., Tanré, D., Deuzé, J.L., Herman, M., and Morcrette, J.J., 1994. *Second Simulation of the Satellite Signal in the Solar Spectrum (6S). User Guide Version 0*, GSFC, NASA, 183 pp.

Vermote, E.F., Tanre, D., Deuze, J.L., Herman, M., and Morcrette, J.J., 1997. Second simulation of the satellite signal in the solar spectrum, 6S - An overview. *IEEE Trans. Geosci. Remote Sens.* 35(3):675-686.

# Appendix

## A General description of the computer code

A rough flowchart of the computer code is in Fig. 1, and the full call-tree in Fig. 2.

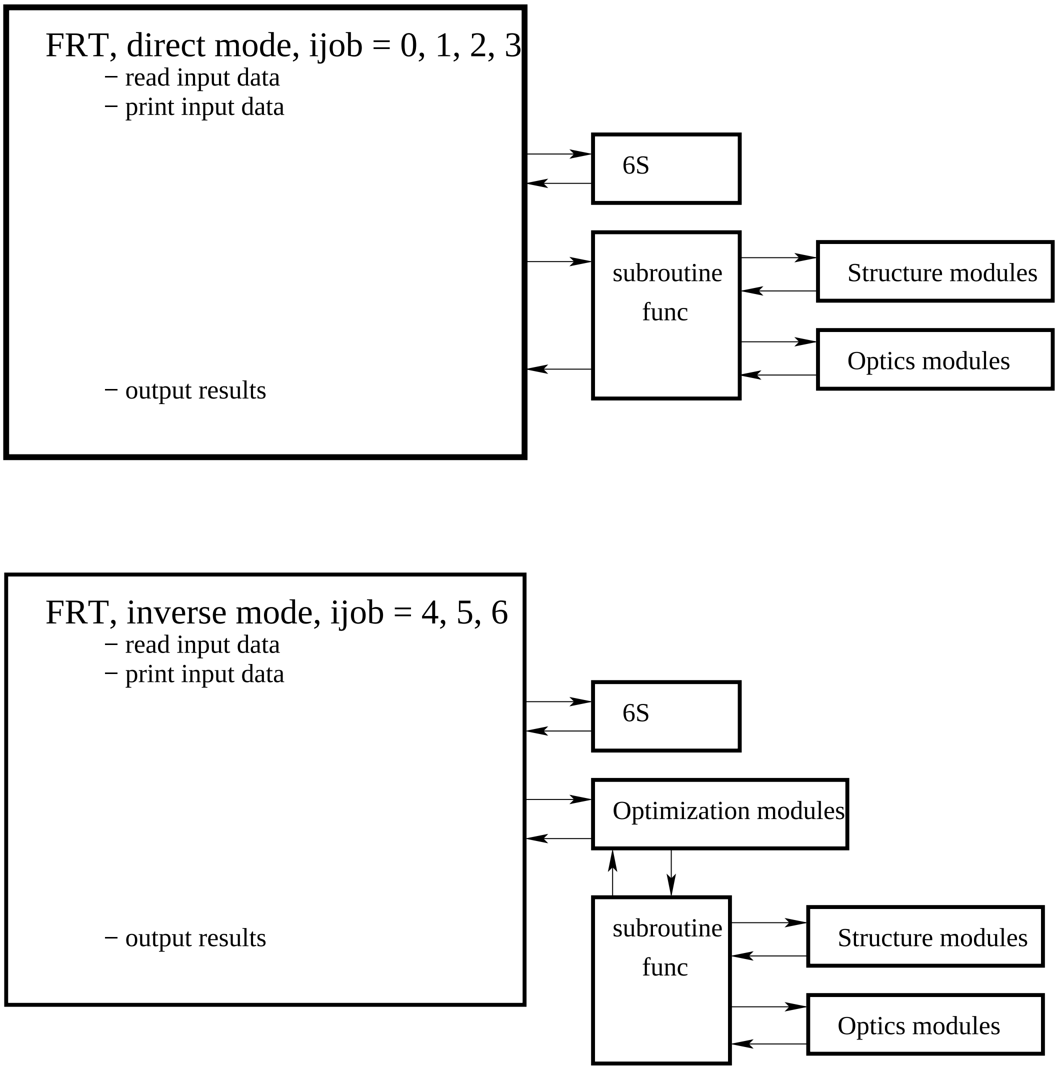


Figure 1: Flowchart of the computer code.

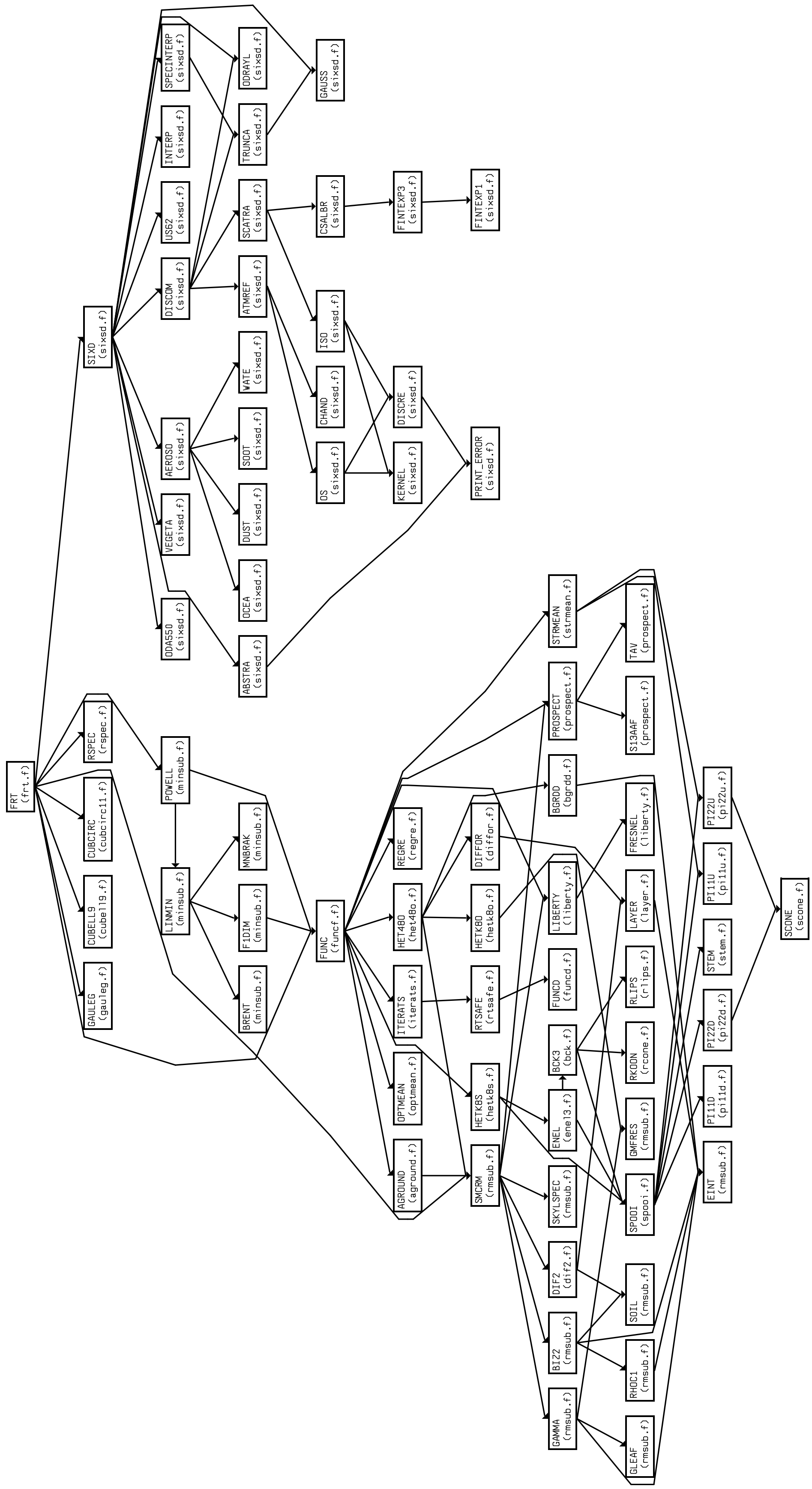


Figure 2: The call-tree of the computer code.

# B The usage

The model is distributed as a compressed tar-archive of source texts, sample input and output files. It is recommended to create a separate directory for the model. Move the archive frt??????.tar.gz to this directory, extract the files and make

```
tar -xzvf frt??????.tar.gz
make frt13    or    make all
```

make clean     removes object files,
make distclean   removes object files and executables.

If you don't use the gfortran compiler then you should modify the makefile.

To run the code type on the commandline

```
./frt13 inputfile outputfile
```

If you do not give input and output files on commandline then you will be asked for the filenames.

Program frt13 calculates in direct mode forest reflectance and transmittance. There are options to perform calculations in various modes:

- a single run for given Sun and view angles and fixed wavelength
- reflectance spectrum for given view and Sun angles in the given range of wavelengths or for a list of spectral bands
- angular distribution of reflectance at given azimuth (relative to the Sun azimuth) for a given Sun zenith angle in the range of view polar angles 0 .. 80°
- BRF in the given direction for the listed Sun angles

Any view and Sun angle is allowed, however, do not use polar angles very close to 90°.

There are several input files required: a file of stand parameters (the stand file), the files of tree parameters for the second, third *etc* tree classes, files of absorption spectra for the leaf optics model, and files of bark and trunk reflectance spectra.

The same code is used for the inversion: parameters of the first tree class and/or ground vegetation can be estimated. An additional flow control file *flow.dat* is required for the model inversion.

## B.1 The stand file

The same stand file can be used both for the direct and inverse modes, however, in the direct mode some input parameters may be missing. The files of the second and other tree classes have the same structure as the stand file for the direct mode, the redundant data may be missing, in case they are present they are not used.

The input parameter $ijob$ controls which task will be run:

| ijob | task |
|---|---|
| 0 | single run, Sun and view angles, and wavelength fixed to the first value of the respective parameter in the input file |
| 1 | calculate spectrum, Sun and view angles fixed |
| 2 | calculate angular distribution for theta = -80 .. 80°, Sun zenith, azimuth and wavelength fixed |
| 3 | $n\_sun$ Sun zenith angles, view angles and wavelength fixed |
| 4 | inversion of the model using BRF values in the fixed view direction, the initial guess, the recommended range of parameters, and errors of the reflectance values are accounted for in the merit function; BRF values at different wavelengths and at different sun angles can be used |
| 5 | inversion of the model, absolute differences in the merit function |
| 6 | inversion of the model using BRF values in various view directions |

**ijob = 1**
The spectral range is determined by the wavelength of the first spectral channel, the wavelength increment $dwl$, and the number of spectral channels. The valid range of wavelengths is 400 - 2400 nm, spectral resolution 1 nm. The spectrum step is given by an input parameter $dwl$, if $dwl \leq 0$ then the list of wavelengths should be given.

**ijob = 2**
Program calculates the angular distribution of forest reflectance and transmittance in the range -80 .. 80° at a given azimuth (relative to the principal plane) and given increment in the view nadir angle. Negative polar angles correspond to the backscattering (hot-spot side), and positive polar angles - to the forward scattering.

**ijob = 3**
Program calculates the forest reflectance at the given view direction for $n\_sun$ Sun zenith angles.

**ijob = 4**
The code is run in inverse mode, $n$ parameters of the first tree class which are listed in the key vector $ll(n)$ are estimated by minimizing the merit function $F(X)$, Eq. (23).

**ijob = 5**
As $ijob = 4$, except absolute differences are accounted for in the merit function $F(X)$, i.e. $\epsilon = 1$ in Eq. (23).

**ijob = 6**
As $ijob = 4$, except sun zenith angle and wavelength are fixed. The section of measured reflectance values differs from that of $ijob = 4$.

## Structure of the stand file

A sample stand file is printed in the page 20. Colons are used to mark comments, information after a colon is not used by the computer program. Below the sample stand file is commented linewise. The row of the input file is printed in bold. As the number of lines is not constant - it depends on the number of leaf components - the lines in comments are not numbered.

## A sample stand file

’Järvselja 112 Pine’ : data set name
124 : stand age
2 : # of size classes
*** files of refractive index and other tree classes ***
’refrind.dat’ ’bepe’

| x0 | xmin | xmax | dx | | i |
|---|---|---|---|---|---|
| ’pine’ | | | | : species | |
| t_elli | | | | : crown form | |
| .1115 | .0001 | .08 | .02 | : stand density, $m^{-2}$ | 1 |
| 15.9 | 10. | 25. | 5. | : tree height, m | 2 |
| 4.2 | .5 | 10. | 9. | : crown l, m; ell \| con | 3 |
| 0. | .5 | 10. | 1. | : cylinder | 4 |
| 1.5 | .2 | 5. | .3 | : crown radius, m | 5 |
| 18. | 2. | 25. | 5. | : trunk diameter, cm | 6 |
| 2.67 | 1.1 | 3. | 8. | : m - total dry leaf weight, kg/tree | 7 |
| 160. | 30. | 180. | 60. | : SLW - leaf weight per area, g m-2 | 8 |
| 3.99 | .0 | 4.5 | .5 | : eln3 - -ln(1 - eps) | 9 |
| 53.57 | 0. | 90. | 20. | : thm3 - modal leaf angle | 10 |
| .1 | .05 | .6 | .2 | : shoot length, m | 11 |
| .3123 | .01 | 1. | .05 | : BAI/LAI | 12 |
| 1.69 | .6 | 2.8 | .05 | : tree distr. param. $GI_j$ | 13 |
| .4 | .1 | .6 | .05 | : H-G asymmetry (phase function) | 14 |
| .6 | | | | : shoot shading coef | |
| ’prospect’ | | | | : leaf optics model | |
| 4 | | | | : # of leaf components | |
| 240. | 50. | 320. | 50. | ’waterb.dat’ : c1, % of SLW, component 1 | 15 |
| .5540 | .3 | 1. | .2 | ’chlorp3.dat’ : c2, % of SLW, component 2 | 16 |
| 97.11 | 94. | 99.8 | 20. | ’drymatter.dat’ : c3, % of SLW, component 3 | 17 |
| 18.91 | 0. | 40.0 | 20. | ’base.dat’ : c4, % of SLW, component 4 | 18 |
| 1.6016 | 1.6 | 2.8 | .5 | : leaf str. param. - PROSPECT N | 27 |
| .9 | .6 | 1.2 | .2 | : refr. ind. ratio | 28 |
| ’pine_branch_1.dat’ | | | | : file of branch reflectance | |
| ’pinetr1.dat’ | | | | : file of trunk reflectance | |
| *** Ground vegetation *** | | | | | |
| .208 | .01 | 6. | .3 | : LAI2_ground, upper layer | 29 |
| .15 | .02 | .4 | .05 | : sl2 - HS-parameter | 30 |
| 1.0 | .4 | 1. | .2 | : clmp2 - foliage clumping parameter | 31 |
| 1.2 | 0. | 2. | .3 | : szz - the displacement parameter | 32 |
| 3.99 | .0 | 4.5 | .5 | : eln2 - -ln(1 - eps) | 33 |
| 53.37 | 0. | 90. | 20. | : thm2 - modal leaf angle | 34 |
| .991 | .6 | 1.3 | .2 | : n_ratio2 | 35 |
| 81.7 | 80. | 180. | 30. | : SLW2($g/m^2$) | 36 |
| ’prospect’ | | | | : leaf optics model, upper layer | |
| 4 | | | | : # of leaf components | |
| 139. | 130. | 320. | 50. | ’waterb.dat’ : c1, % of SLW, component 1 | 37 |
| .36 | .3 | .8 | .2 | ’chlorp3.dat’ : c2, % of SLW, component 2 | 38 |
| 99.52 | 94. | 99.8 | 20. | ’drymatter.dat’ : c3, % of SLW, component 3 | 39 |
| .10 | .0002 | 4. | .1 | ’brownpigm.dat’ : c4, % of SLW, component 4 | 40 |
| 1.315 | 1. | 2.8 | .2 | : N2 (PROSPECT) | 49 |
| 1.064 | .01 | 1.1 | .3 | : LAI1_ground, lower layer | 50 |
| .15 | .02 | .4 | .05 | : sl1 - HS-parameter | 51 |
| 1. | .4 | 1. | .2 | : clmp1 - foliage clumping parameter | 52 |
| 3.0 | .0 | 4.5 | .5 | : eln1 - -ln(1 - eps) | 53 |
| 75.469 | 0. | 90. | 20. | : thm1 - modal leaf angle | 54 |
| 1.224 | .6 | 1.3 | .2 | : n_ratio1 | 55 |
| 78.54 | 70. | 180. | 30. | : SLW1($g/m^2$) | 56 |
| ’prospect’ | | | | : leaf optics model, lower layer | |
| 5 | | | | : # of leaf components | |
| 134.24 | 130. | 320. | 50. | ’waterb.dat’ : c1, % of SLW, component 1 | 57 |
| .425 | .3 | .8 | .2 | ’chlorp3.dat’ : c2, % of SLW, component 2 | 58 |
| 0.733 | .3 | .8 | .2 | ’anthocyanins.dat’ : c3, % of SLW, component 3 | 59 |
| 98.343 | 94. | 99.8 | 20. | ’drymatter.dat’ : c4, % of SLW, component 4 | 60 |

```
.50         .0002     4.        .1      'cellp3.dat' : c5, % of SLW, component 5      61
1.0053      1.        2.5       .2           : N1 (PROSPECT)                          69
'soil.dat'  45.                              : file of Price' vectors, th*
2.0373      .05       .4        .07          : s1 - soil parameters                   70
.0          -.1       .1        .02          : s2                                     71
.0          -.05      .05       .02          : s3                                     72
.0          -.04      .04       .02          : s4                                     73
4           .80  .17  .0  .03   : iaer, c(i) - aerosol data (6S)
0.          .09                          : v, tau_aer(550) - visibility (6S)
1           : *ijob*: 0-single, 1-spectrum, 2-ad, 3-n_sun, 4,5,6-inversion (4-relat., 5-abs. differences, 6-BRF)
1           6         -1.                : # of Sun angles, spectral bands/BRF values, spectrum step
37.6  50.                                : Sun zeniths
486. 571. 650. 838. 1677. 2217.          : spectral bands (TM)
0.          2.        0.                 : view nadir angle, its increment, and azimuth angle
'powell'                                 : name of the optimization subroutine
5000        1         100       100      : nfmax, itmax, itbr, nbrak
1.E-9       1.E-7     1.E-13    1.E-8    : zeps, tolbr, tiny, ftolp
1.          .5        2.        .2       : alpha, beta, gamma, dx
2           20.       f                  : n, at, lig - which initial guess
1           7                            : ll(i)
486.        .0271     .02                : th_Sun=37.6
572.        .2744     .1                 : th_Sun=37.6
661.        .2806     .1                 : th_Sun=37.6
838.        .0228     .02                : th_Sun=50.
1677.       .2702     .1                 : th_Sun=50.
2217.       .2765     .1                 : th_Sun=50.
**********************************************************
lambda      reflectance  delta_rho
```

**'Järvselja 112 Pine'** : data set name
**124** : stand age
**2** : # of size classes

The number of tree classes, the max number of tree classes is 10.

***** files of refractive index and other tree classes ***** – a comment line
**'refrind.dat' 'bepe'**

This line cannot be omitted in the case of one tree class.

**x0** **xmin** **xmax** **dx** **i** - a comment
**'pine'** : tree species, a character string for information purposes only
**t_elli** : crown form,

A logical parameter of crown shape: t – ellipsoid, f – cylinder+cone

Starting from the next row there are four parameter values in each line. Only the first value (*x0*) is required for the direct problem, $x\_min$ and $x\_max$ are the boundary values of the parameter in the inversion run. The fourth column, $dx$, is the tolerance of the parameter in the inversion, Eq. (23). The first value (*x0*) serves as an initial guess and as an expert estimate $x_{e,j}$, Eq. (23) of the parameter value in the inversion. There is the parameter number in the vector of parameters in the last column. Only the first column (*x0*) is needed in the direct mode ($ijob$ = 0, 1, 2, 3)

**.1115** **.0001** **.08** **.08** : stand density, m$^{-2}$

Number of trees for the given tree class

**15.9** **10.** **25.** **5.** : tree height, m

| | | | | |
|---|---|---|---|---|
| **4.2** | **.5** | **10.** | **9.** | : crown l, m; ell \| con |

Crown length (ellipsoid) or length of the conical part of the crown (cylinder+cone)

| | | | | |
|---|---|---|---|---|
| **0.** | | | | : cylinder |

Length of the cylindrical part of crown

| | | | | |
|---|---|---|---|---|
| **1.5** | **.2** | **5.** | **.3** | : crown radius, m |

Crown radius - the horizontal semiaxis of ellipsoid or the base radius of the cone

| | | | | |
|---|---|---|---|---|
| **18.** | **2.** | **25.** | **5.** | : trunk diameter, cm |

$DBH$ – trunk diameter at the breast height.

| | | | | |
|---|---|---|---|---|
| **2.67** | **1.1** | **3.** | **8.** | : m - total dry leaf weight, kg/tree |
| **160.** | **30.** | **180.** | **60.** | : SLW - leaf weight per area, g m-2 |
| **3.99** | **.0** | **4.5** | **.5** | : eln3 - -ln(1 - eps) |

the eccentricity parameter of LAD

| | | | | |
|---|---|---|---|---|
| **53.57** | **0.** | **90.** | **20.** | : thm3 - modal leaf angle |
| **.1** | **.05** | **.6** | **.2** | : shoot length, m |
| **.3123** | **.01** | **1.** | **.05** | : BAI/LAI ratio |
| **1.69** | **.6** | **2.8** | **.05** | : tree distr. param. $GI_j$ |

Grouping index, $GI_j = 1$ – a random stand, $GI_j < 1$ – a clumped stand, $GI_j > 1$ – a regular stand.

| | | | | |
|---|---|---|---|---|
| **.4** | **.1** | **.6** | **.05** | : H-G asymmetry (phase function) |

If this parameter is $\leq 0$, then the Ross-Nilson area scattering phase function of plate medium is used.

| | | | | |
|---|---|---|---|---|
| **.6** | | | | : shoot shading coef |

Shoot shading parameter $\kappa$, accounts for the decrease of effective G-function due the mutual shading of leaves (needles) , $\kappa = 1$ – no mutual shading.

| | |
|---|---|
| **'prospect'** | : leaf optics model, options are 'prospect' and 'liberty'. |
| **4** | : # of leaf components $n_{comp}$ |

In the next $n_{comp}$ lines the percent concentration of the component and the file name of the component absorption spectrum for every component is listed. Despite in the direct mode only the first parameter $x(0)$ is used, the filename must be at the fifth position in the line. The components 15-24 of the vector of parameters are reserved for the leaf biochemical constituents - the tree layer, components 37-46 - the upper layer of ground vegetation, and components 57-66 - the lower layer of ground vegetation, so the maximum number of leaf biochemical components is 10. The components 25 and 26, 47 and 48, and 67 and 68 of the vector of parameters are the LIBERTY parameters cell diameter and amount of inter-cell air, for the tree layer, the upper and lower layer of ground vegetation, respectively.

| | | | | | |
|---|---|---|---|---|---|
| **.1** | **.3** | **1.** | **.2** | **'chlorp3.dat'** | : c1, % of SLW, model component 1 |
| **250.** | **50.** | **320.** | **50.** | **'waterp3.dat'** | : c2, % of SLW, model component 2 |
| **99.8** | **94.** | **99.9** | **20.** | **'drymatter.dat'** | : c3, % of SLW, model component 3 |
| **1.6016** | **1.6** | **2.8** | **.5** | | : leaf str. param. - - PROSPECT N |
| **1.** | **.6** | **1.2** | **.2** | | : refr. ind. ratio |

Refraction index of the leaf surface wax is calculated from the tabulated value by multiplying to this coefficient.

| | | | | |
|---|---|---|---|---|
| **.4** | **.1** | **.6** | **.2** | : shoot length, m |
| **’pine_branch_1.dat.dat’** | | | | : file of branch reflectance |
| **’pinetr.dat’** | | | | : file of trunk reflectance |

The next group of parameters are the input parameters of the two-layer CR model (Kuusk, 2001).

| | | | | |
|---|---|---|---|---|
| ****** Ground vegetation ***** | | | - a comment | |
| **.59** | **.01** | **6.** | **6.** | : LAI2_ground, upper layer |
| **.15** | **.02** | **.4** | **.4** | : sl2 - HS-parameter |
| **1.0** | **.4** | **1.** | **.2** | : clmp2 - foliage clumping parameter |
| **1.2** | **0.** | **2.** | **.3** | : szz - the displacement parameter |
| **3.99** | **.0** | **4.5** | **.5** | : eln2 - -ln(1 - eps) |
| **53.37** | **0.** | **90.** | **20.** | : thm2 - modal leaf angle |
| **.9** | **.6** | **1.3** | **.2** | : n_ratio2 |
| **78.** | **80.** | **180.** | **30.** | : SLW2($g/m^2$) |
| **’prospect’** | | | | : leaf optics model, upper layer |
| **4** | | | | : # of leaf components |
| **.4** | **.3** | **.8** | **.2** | **’chlorp3.dat’** : c1, % of SLW, component 1 |
| **150.** | **130.** | **320.** | **50.** | **’waterp3.dat’** : c2, % of SLW, component 2 |
| **99.6** | **94.** | **99.8** | **20.** | **’drymatter.dat’** : c3, % of SLW, component 3 |
| **.2** | **.0002** | **4.** | **.1** | **’brownpigm.dat’** : c4, % of SLW, component 4 |
| **1.315** | **1.** | **2.8** | **.2** | : N2 (PROSPECT) |
| **.1** | **.01** | **1.** | **1.** | : LAI1_ground, lower layer |
| **.15** | **.02** | **.4** | **.4** | : sl1 - HS-parameter |
| **1.** | **.4** | **1.** | **.2** | : clmp1 - foliage clumping parameter |
| **0.** | **.0** | **4.5** | **.5** | : eln1 - -ln(1 - eps) |
| **90.** | **0.** | **90.** | **20.** | : thm1 - modal leaf angle |
| **.9** | **.6** | **1.3** | **.2** | : n_ratio1 |
| **78.** | **80.** | **180.** | **30.** | : SLW1($g/m^2$) |
| **’prospect’** | | | | : leaf optics model, lower layer |
| **4** | | | | : # of leaf components |
| **.4** | **.3** | **.8** | **.2** | **’chlorp3.dat’** : c1, % of SLW, component 1 |
| **150.** | **130.** | **320.** | **50.** | **’waterp3.dat’** : c2, % of SLW, component 2 |
| **99.6** | **94.** | **99.8** | **20.** | **’drymatter.dat’** : c3, % of SLW, component 3 |
| **.2** | **.0002** | **4.** | **.1** | **’brownpigm.dat’** : c4, % of SLW, component 4 |
| **1.0053** | **1.** | **2.5** | **.2** | : N1 (PROSPECT) |
| **’price.dat’** | **45.** | | | : file of Price’ vectors, th* |
| **.217** | **.05** | **.95** | **.95** | : s1 - soil parameters |
| **-.05** | **-.1** | **.1** | **.02** | : s2 |
| **.0** | **-.05** | **.05** | **.02** | : s3 |
| **.0** | **-.04** | **.04** | **.02** | : s4 |

The next group of parameters are the input parameters of the 6S model (Vermote et al., 1997).

**2** **.70 .29 0. .01** : iaer, c(i) - aerosol data (6S)

$iaer, c(i)$ – aerosol model (6S)
-1 BRDF, no sky radiation
0 no aerosols
1 continental model
2 maritime model
3 urban model
4 enter the volumic percentage of each component $c(i)$
$c(1)$ – fraction of dust-like
$c(2)$ – water-soluble
$c(3)$ – oceanic
$c(4)$ – soot

**30.** **.060** : visibility $v$, km, and/or tau_aerosol(550 nm) if $v$< 0
**1** : *ijob*: 0-single, 1-spectrum, 2-ad, 3-n_sun,
4,5,6-inversion (4-relat., 5-abs. differences, 6-BRF)

The job control parameter $ijob$:
0 - calculate a single value of canopy reflectance
1 - calculate reflectance spectrum for the given Sun and view angles
2 - calculate reflectance angular distribution at given azimuth
3 - calculate CR for several Sun zenith angles
4 - inversion of the FRT model, relative differences in the merit function
5 - inversion of the FRT model, absolute differences in the merit function
6 - inversion of the FRT model, BRF values in different view directions

**2** **3** **-5.** : # of Sun angles, spectral bands, spectrum step

Number of Sun angles and spectral bands; the spectrum step $d\lambda$. If $d\lambda < 0$ then give the list of spectral bands on the next line. Otherway, the spectrum has the fixed increment and only the first wavelength is read.
**NB!** In case of inversion $\mathbf{ijob = 6}$, the second parameter in this line is the number of given BRF values. Up to 2000 spectral bands ($ijob = 1$) or given reflectance values in the inversion $ijob = 6$ are allowed.

**20.** **50.** : Sun zeniths
**675.** **800.** **1360.** : spectral bands
**0.** **2.** **0.** : view nadir angle, its increment, and azimuth angle.
The azimuth angle is counted from the principal plane.

The next group of parameters are optimization parameters. The only working option for the optimization subroutine is 'powell'.

**'powell'** : name of the optimization subroutine
**5000** **1** **100** **100** : nfmax, itmax, itbr, nbrak
$nfmax$ – the max number of calculations of merit function
$itmax$ – the max number of iterations
$itbr$ – the max number of iterations in the subroutine brent
$nbrak$ – number of iterations in the subroutine mnbracket
**1.E-9** **1.E-7** **1.E-13** **1.E-8** : zeps, tolbr, tiny, ftolp

| | | | | |
|---|---|---|---|---|
| **1.** | **.5** | **2.** | **.2** | : alpha, beta, gamma, dx |
| **2** | **10.** | **f** | | : n, at, lig - which initial guess |

$n$ - the number of model parameters subject to inversion
$at$ - penalty – the weight $w_i$, Eq. (23), at = 10. is ok!
$lig$ is a logical parameter,
$lig$ = t (.true.) – parameters will be read from a temporary file
(results of the previous iteration)
$lig$ = f (.false.) – parameters will be read from the input file
In the first run take $lig$ = f (.false.)

| | | | | |
|---|---|---|---|---|
| **11** | **14** | | | : ll(i) |

The key vector $ll(n)$, here the ordinal numbers of free model parameters which are subject to estimation are listed.

The next lines are the reflectance values for inversions $ijob = 4$ and $ijob = 5$: for the first Sun zenith for every spectral channel, for the second Sun zenith for every spectral channel etc. The number of reflectance/transmittance values should be $n\_chnl * n\_sun$.

| | | | |
|---|---|---|---|
| **675.** | **.0271** | **.02** | : th_Sun=37.6 |
| **800.** | **.2744** | **.1** | : th_Sun=37.6 |
| **1360.** | **.2806** | **.1** | : th_Sun=37.6 |
| **675.** | **.0228** | **.02** | : th_Sun=50. |
| **800.** | **.2702** | **.1** | : th_Sun=50. |
| **1360.** | **.2765** | **.1** | : th_Sun=50. |

In the inversion $ijob = 6$ the structure of this group of data is different. The columns are

VZA VAA BRF

Here, VZA and VAA are the view zenith and azimuth angles, respectively. The ranges are 0..90 and -180..180, respectively. The view azimuth angle is counted from the sun azimuth.

## B.2 A sample file of the second tree class

| | |
|---|---|
| 'Järvselja Pine' | : data set name |
| 124 | : stand age |
| 2 | : # of size classes |
| ** files of refractive index and other tree classes: | |
| 'refrind.dat' 'bepe' | |
| x0 | |
| 'KS' | : species |
| t_elli | : crown form |
| .0006 | : stand density, $m^{-2}$ |
| 4.1 | : tree height, m |
| 2.9 | : crown l, m; ell \| con |
| 0. | : cylinder |

| | | | | |
|---|---|---|---|---|
| 0.8 | | | | : crown radius, m |
| 5.5 | | | | : trunk diameter, cm |
| 0.6 | | | | : m - total leaf weight, kg/tree |
| 76. | | | | : SLW - leaf weight per area, g m-2 |
| 0. | | | | : eln3 - -ln(1 - eps) |
| 53.57 | | | | : thm3 - modal leaf angle |
| .2 | | | | : shoot length, m |
| .1505 | | | | : BAI/LAI |
| 1.69 | | | | : tree distr. param. $GI_j$ |
| 0. | | | | : H-G asymmetry (phase function) |
| .95 | | | | : shoot shading coef |
| ’prospect’ | | | | : leaf optics model |
| 4 | | | | : # of leaf components |
| 76.6 | 50. | 320. | 50. | ’waterb.dat’ : c1, % of SLW, component 1 |
| .7375 | .3 | 1. | .2 | ’chlorp3.dat’ : c2, % of SLW, component 2 |
| 99.9 | 94. | 99.8 | 20. | ’drymatter.dat’ : c3, % of SLW, component 3 |
| 7.395 | 0. | 40.0 | 20. | ’base.dat’ : c4, % of SLW, component 4 |
| 1.548 | 1.05 | 2.5 | .2 | : leaf str. param. - PROSPECT N |
| .9 | .6 | 1.2 | .2 | : refr. ind. ratio |
| ’birch_branch_1.dat’ | | | | : file of branch reflectance |
| ’birctr1.dat’ | | | | : file of trunk reflectance |

## B.3 The flow control file *flow.dat*

The inversion procedure is iterative. If in given number of iterations the minimum of the merit function is found, $ier = 1$, then the program prints output and stops. Otherway ($ier \neq 1$), the flow control parameter $next$ is read from the flow control file *flow.dat*. The meaning of this parameter is:

1 - continue
7 - stop

### A sample file *flow.dat*

1 : continue
1 : continue
1 : continue
7 : stop

## B.4 Bark and trunk reflectance spectra

The files of bark and trunk reflectance spectra are simple two-column files of 2001 rows, where the first column is wavelength, nm, and the second column is reflectance. The wavelength interval is 1 nm.

## C A sample output file

```
#
#   Forest Reflectance Model V.04.2013
#   by A. Kuusk, T. Nilson
#
# Input parameters:
#   Stand Age  =  124     Järvselja Pine
##  ijob =   1
#   Sun zenith =  37.0  View zenith =   0.0  View azimuth =   0.0
#     16 spectral bands
#   Files of parameters of other tree classes:
#   bepe
#                        MA      KS
#                        ellips  ellips
#   stand density, m-2   0.1115  0.0006
#   tree height, m       15.900   4.100
#   ellipsoid or cone     4.200   2.900
#   cylinder, m           0.000   0.000
#   crown radius, m       1.500   0.800
#   trunk diameter, cm   18.000   5.500
#   total leaf weight     2.670   0.598
#   leaf weight, g m-2  160.000  76.000
#   eln                   3.990   0.000
#   thm                  53.570  53.570
#   shoot size, m         0.100   0.200
#   BAI/LAI               0.312   0.150
#   tree distr. param.    1.690   1.690
#   g_H-G                 0.400   0.000
#  Shoot clumping:        0.600   0.950
#   Leaf models:           prospect          prospect
#   # of leaf componen        4       4
#      waterb.dat        waterb.dat
#   c1, % of SLW         240.00   76.60
#      chlorp3.dat       chlorp3.dat
#   c2, % of SLW           0.55    0.74
#      drymatter.dat     drymatter.dat
#   c3, % of SLW          97.11   99.90
#      base.dat          base.dat
#   c4, % of SLW          18.91    7.36
#   leaf str.par         1.6016  1.5480
#   refr. ind. ratio     0.9000  0.9000
#   bark refl. files:  pine_branch_1.dat          birch_branch_1.dat
#   trunk refl. files  pinetr1.dat                birctr1.dat
#
# *** Ground vegetation, upper layer
#   ground LAI             0.21
#   leaf size              0.15
#   clmp                   1.00
#   szz                    1.20
#   eln                    3.99
#   thm                   53.57
#   n_ratio                0.99
#   SLW                   81.70
#   Leaf model:     prospect
#   # of leaf components:     4
#      waterb.dat
#   c1, % of SLW         139.08
#      chlorp3.dat
#   c2, % of SLW           0.36
#      drymatter.dat
#   c3, % of SLW          99.52
```

```
#      brownpigm.dat
#   c4, % of SLW          0.10
#   leaf str.par        1.3150
# *** Ground vegetation, lower layer
#   ground LAI            1.06
#   leaf size             0.15
#   clmp                  1.00
#   eln                   3.00
#   thm                  75.47
#   n_ratio               1.22
#   SLW                  78.54
#   Leaf model:     prospect
#   # of leaf components:     5
#      waterb.dat
#   c1, % of SLW        134.24
#      chlorp3.dat
#   c2, % of SLW          0.42
#      anthocyanins.dat
#   c3, % of SLW          0.73
#      drymatter.dat
#   c4, % of SLW         98.34
#      cellp3.dat
#   c5, % of SLW          0.50
#   leaf str.par        1.0053
#   s1_soil             2.0373
#   s2                  0.0000
#   s3                  0.0000
#   s4                  0.0000
#
# 6S parameters
#          aerosols type identity : user defined aerosols model         *
#                                 0.800 % of dust-like                  *
#                                 0.170 % of water-soluble              *
#                                 0.000 % of oceanic                    *
#                                 0.030 % of soot                       *
#                       optical condition identity :                    *
#            visibility  72.64 km  opt. thick. 550nm  0.0900            *
#                     ground pressure [mb] 1013.00                      *
#
# *** Results:
#                             1         2
#                            MA        KS      totals
#                         ellips    ellips
#   stand density, m-2      0.112     0.001     0.112
#   tree height, m         15.900     4.100    15.837
#   ellipsoid or cone       4.200     2.900     4.193
#   cylinder, m             0.000     0.000     0.000
#   crown radius, m         1.500     0.800     1.496
#   trunk diameter, cm     18.000     5.500    17.933
#   total leaf weight       2.670     0.598     2.659
#   leaf weight, g m-2    160.000    76.000   159.550
#   eln                     3.990     0.000     0.000
#   thm                    53.570    53.570     0.000
#   shoot size, m           0.100     0.200     0.000
#   BAI/LAI                 0.312     0.150     0.582
#   tree distr. param.      1.690     1.690     0.000
#   g_H-G                   0.400     0.000     0.000
#  Shoot clumping:          0.600     0.950
#  Leaf models:     prospect    prospect
#  # of leaf components        4         4
#      waterb.dat        waterb.dat
#   c1, % of SLW          240.00     76.60
#      chlorp3.dat       chlorp3.dat
#   c2, % of SLW            0.55      0.74
```

```
#      drymatter.dat     drymatter.dat
#   c3, % of SLW            97.11     99.90
#      base.dat          base.dat
#   c4, % of SLW            18.91      7.36
#   leaf str.par           1.6016    1.5480
#   bark refl. files:  pine_branch_1.dat         birch_branch_1.dat
#   trunk refl. files  pinetr1.dat               birctr1.dat
#   rl_eff =  0.0803  tl_eff =  0.0009  n_eff =  1.3408  rsl =  0.1131
#   leaf area density       0.769     2.228
#   Total LAI     1.865
#   Total BAI     0.582
#   crown closure =  0.789        canopy closure =  0.737
#
#  *** Ground vegetation, upper layer
#   ground LAI                0.21
#   leaf size                 0.15
#   clmp                      1.00
#   szz                       1.20
#   eln                       3.99
#   thm                      53.57
#   n_ratio                   0.99
#   SLW                      81.70
#   Leaf model:   prospect
#   # of leaf components:       4
#      waterb.dat
#   c1, % of SLW            139.08
#      chlorp3.dat
#   c2, % of SLW              0.36
#      drymatter.dat
#   c3, % of SLW             99.52
#      brownpigm.dat
#   c4, % of SLW              0.10
#     leaf str.par         1.3150
#  *** Ground vegetation, lower layer
#   ground LAI                1.06
#   leaf size                 0.15
#   clmp                      1.00
#   szz                       3.00
#   eln                      75.47
#   thm                       1.22
#   n_ratio                  78.54
#   Leaf model:   prospect
#   # of leaf components:       5
#      waterb.dat
#   c1, % of SLW            134.24
#      chlorp3.dat
#   c2, % of SLW              0.42
#      anthocyanins.dat
#   c3, % of SLW              0.73
#      drymatter.dat
#   c4, % of SLW             98.34
#      cellp3.dat
#   c5, % of SLW              0.50
#   leaf str.par           1.0053
#   s1_soil                2.0373
#   s2                     0.0000
#   s3                     0.0000
#   s4                     0.0000
#
#   Järvselja Pine
#   Sun zenith =  37.0  View zenith =   0.0  View azimuth =   0.0
#     16 spectral bands
# wl, nm  refl.   b_down   r_ground   S’/Q     rcr1       rgr1       rdif
#
```

| | | | | | | | |
|---|---|---|---|---|---|---|---|
| 489.1 | 0.1788E-1 | 0.1006 | 0.4421E-1 | 0.8343 | 0.7020E-2 | 0.7104E-2 | 0.3754E-2 |
| 528.6 | 0.3449E-1 | 0.9900E-1 | 0.7035E-1 | 0.8628 | 0.1604E-1 | 0.1128E-1 | 0.7161E-2 |
| 549.7 | 0.3986E-1 | 0.9643E-1 | 0.8026E-1 | 0.8758 | 0.1886E-1 | 0.1293E-1 | 0.8063E-2 |
| 568.2 | 0.3740E-1 | 0.8890E-1 | 0.7871E-1 | 0.8859 | 0.1753E-1 | 0.1278E-1 | 0.7079E-2 |
| 629.1 | 0.3296E-1 | 0.7337E-1 | 0.7529E-1 | 0.9088 | 0.1521E-1 | 0.1243E-1 | 0.5303E-2 |
| 658.6 | 0.3028E-1 | 0.6709E-1 | 0.7415E-1 | 0.9170 | 0.1355E-1 | 0.1234E-1 | 0.4377E-2 |
| 671.9 | 0.2994E-1 | 0.6502E-1 | 0.7506E-1 | 0.9208 | 0.1325E-1 | 0.1252E-1 | 0.4159E-2 |
| 694.5 | 0.4145E-1 | 0.7074E-1 | 0.9557E-1 | 0.9257 | 0.1906E-1 | 0.1585E-1 | 0.6537E-2 |
| 703.4 | 0.6282E-1 | 0.8437E-1 | 0.1356 | 0.9276 | 0.2861E-1 | 0.2227E-1 | 0.1193E-1 |
| 709.5 | 0.8319E-1 | 0.9984E-1 | 0.1635 | 0.9295 | 0.3826E-1 | 0.2663E-1 | 0.1829E-1 |
| 738.5 | 0.1789 | 0.1729 | 0.2718 | 0.9355 | 0.7438E-1 | 0.4302E-1 | 0.6157E-1 |
| 748.6 | 0.2001 | 0.1881 | 0.2920 | 0.9373 | 0.8069E-1 | 0.4602E-1 | 0.7345E-1 |
| 777.2 | 0.2188 | 0.1980 | 0.3143 | 0.9422 | 0.8529E-1 | 0.4947E-1 | 0.8412E-1 |
| 867.8 | 0.2466 | 0.2059 | 0.3622 | 0.9521 | 0.8920E-1 | 0.5710E-1 | 0.1003 |
| 890.8 | 0.2526 | 0.2070 | 0.3729 | 0.9547 | 0.8999E-1 | 0.5883E-1 | 0.1038 |
| 905.1 | 0.2562 | 0.2075 | 0.3796 | 0.9563 | 0.9046E-1 | 0.5993E-1 | 0.1058 |

# D Description of the subroutines

## D.1 Subroutines of general use

### D.1.1 Function *func*

**Function:** In the direct mode the function *func* organizes the data exchange between subroutines and the main program.

In the inverse mode the function *func* checks that the model parameters are in the allowed range, organizes the data exchange between subroutines and the main program, and computes the merit function.

### D.1.2 Subroutines *iterats, rtsafe* and *funcd*

**Function:** To compute the Fisher's grouping index $GI_j$, Eq. (10) from the given structure parameter $c_j(\theta_1)$.

**Description:** The Newton-Raphson method is used, Press et al. (1992), Algorithm 9.4.

### D.1.3 Subroutines *cubell9, cubcirc* and *gauleg*

**Function:** Provide quadrature (cubature) knots and weights to numerical integrations

### D.1.4 Subroutine *rspec*

**Function:** Reads tabulated spectra – absorption spectra of leaf constituents, stem and branch bark reflectance, Price' vectors *etc.*

## D.2 Structure modules

### D.2.1 Subroutine *strmean*

**Function:** Computes the mean values of structure parameters.

### D.2.2 Subroutine *regre*

**Function:** Regressions for tree parameters. The call of this subroutine is commented out. Such regressions can be used in case some tree parameters are not available.

### D.2.3 Subroutine *ggg*

**Function:** The Ross-Nilson G-function for elliptical LAD.

### D.2.4 Subroutine *hetk8s*

**Function:** Coordinates the calculation of free lines of sight in Sun and view directions.

### D.2.5 Subroutine *enel*

**Function:** Integrates the bidirectional probability $p_{00j}$, over the whole tree crown, Eq. (3), and computes the probability to see the sunlight trunk.

**Description:** The volume integral $\int\int\int_{V_j} p_{00j}(x, y, z; r_1, r_2)\, dx\, dy\, dz$ is calculated using a cubature for a sphere (ellipsoid) or cubature for a circle and Gauss-Legendre quadrature in respect of the z-coordinate for a cone+cylinder.

### D.2.6 Subroutine *bck3*

**Function:** Computes the bidirectional gap probability $p_{ooj}$, Eq. (4).

### D.2.7 Subroutine *spooj*

**Function:** Computes the between-crown gap probability $p_2$, Eq. (4).

**Description:** The overlapping of crown projections in Sun and view directions $S_{cj}()$ is calculated so that the crown projections $S_1$ and $S_2$ in Sun and view directions, respectively, are substituted with circles of the same area. Centers of the circles are halfway between the projections of the base and the top of a crown, see Fig. 2 (p. 7).

### D.2.8 Subroutines *rlips* and *rkoon*

**Function:** Subroutines *rlips* and *rkoon* compute the distance from the given point $M(x, y, z)$ to the perimeter of the ellipsoid or cone+cylinder, respectively, in the given direction $(\theta, \varphi)$.

### D.2.9 Subroutines *pi11u, pi11d, pi22u* and *pi22d*

**Function:** Subroutines *pi11u, pi11d, pi22u* and *pi22d* compute projections of the crown part above (*pi11u, pi22u*) and below (*pi11d, pi22d*) the given level $z$.

### D.2.10 Subroutine *scone*

**Function:** Computes the projection area of a cone/frustum of a cone for a given direction.

### D.2.11 Subroutine *stem*

**Function:** Computes the projection area of a stem.

## D.3 Optics modules

### D.3.1 Subroutine *optmean*

**Function:** Computes the mean and effective values of optical parameters.

### D.3.2 Subroutine *aground*

**Function:** Computes the directional-hemispherical reflectance $rsdgrou$ and albedo (hemispherical-hemispherical reflectance) $rddgrou$ of ground vegetation.

**Description:** The double integral over hemisphere which is needed for the hemispherical-hemispherical reflectance of ground vegetation is substituted by an integral over polar angle at the azimuth $\varphi = 90°$. The integral is calculated with an Gaussian quadrature.

### D.3.3 Subroutine *het48o*

**Function:** Computes radiances down and up, and transmittance of the tree layer.

### D.3.4 Subroutine *hetk8o*

**Function:** Sums together radiance of all tree classes.

### D.3.5 Subroutine *diffor*

**Function:** Computes diffuse fluxes of multiple scattering and of scattered diffuse sky radiation.

**Description:** Diffuse fluxes are computed in two-stream approximation (Bunnik, 1978; Kuusk, 2001).

## D.4 Reflectance of ground vegetation

Subroutines

*smcrm*
*biz2*
*gamma*
*gleaf*
*gmfres*
*soil*
*dif2*
*layer*
*rhoc1*
*skylspec*

constitute the two-layer homogeneous canopy reflectance model ACRM. The full description of algorithms is published by Kuusk (1994, 1995a,b, 2001).

## D.5 PROSPECT - the leaf optics model

Subroutines

*prospect*
*tav*
*s13aaf*

constitute the leaf optics model by Jacquemoud and Baret (1990).

## D.6 LIBERTY - the leaf optics model

Subroutines

*liberty*
*fresnel*

constitute the leaf optics model by Dawson et al. (1998).

## D.7 Atmosphere radiative transfer model 6S

General description of the 6S model is published by Vermote et al. (1997). The detail description of 6S modules is in (Vermote et al., 1994). For the calculation of incoming fluxes are used the modules

*sixd*
*abstra*
*aeroso*
*atmref*
*chand*
*csalbr*
*discom*
*discre*
*dust*
*gauss*

*interp*
*iso*
*kernel*
*ocea*
*oda550*
*odrayl*
*os*
*print_error*
*scatra*
*soot*
*specinterp*
*trunca*
*us62*
*vegeta*
*wate*

## D.8 Optimization modules

The Powell's method (Press et al., 1992), Algorithm 10.5 is used for the minimization of the merit function Eq. (16). The corresponding subroutines are

*powell*
*linmin*
*mnbrak*
*function brent*

# References


Bunnik, N.J.J., 1978. *The Multispectral Reflectance of Shortwave Radiation by Agricultural Crops in Relation with their Morphological and Optical Properties*, Mededelingen Landbouwhogeschool, Wageningen, The Netherlands, 175 pp.

Dawson, T.P., Curran, P.J., and Plummer, S.E., 1998. LIBERTY - modeling the effects of leaf biochemical concentration on reflectance spectra. *Remote Sens. Environ.* 65:50-60.

Jacquemoud, S., and Baret, F., 1990. PROSPECT: A model of leaf optical properties spectra. *Remote Sens. Environ.* 34:75-91.

Kuusk, A., 1994. A multispectral canopy reflectance model. *Remote Sens. Environ.* 50:75–82.

Kuusk, A., 1995a. A fast, invertible canopy reflectance model, textit Remote Sens. Environ. 51(3): 342-350.

Kuusk, A., 1995b. A Markov chain model of canopy reflectance. *Agricult. Forest Meteorol.* 76:221–236.

Kuusk, A., 2001. A two-layer canopy reflectance model. *J.Q.S.R.T.* 71:1-9.

Lenoble, J. (Ed.), 1977. *Standard Procedures to Compute Atmospheric Radiative Transfer in a Scattering Atmosphere. Vol. I.* International Association of Meteorology and Atmospheric Physics, Radiation Commission, Boulder, Co. National Center for Atmospheric Research.

Press, W.H., Teukolsky, S.A., Vetterling, W.T., and Flannery, B.P., 1992. *Numerical Recipes in FORTRAN. The Art of Scientific Computing.* Cambridge University Press, Cambridge, 963 pp.

Vermote, E., Tanré, D., Deuzé, J.L., Herman, M., and Morcrette, J.J., 1994. *Second Simulation of the Satellite Signal in the Solar Spectrum (6S). User Guide Version 0*, GSFC, NASA, 183 pp.

Vermote, E.F., Tanre, D., Deuze, J.L., Herman, M., and Morcrette, J.J., 1997. Second simulation of the satellite signal in the solar spectrum, 6S - An overview. *IEEE Trans. Geosci. Remote Sens.* 35(3):675-686.